Finite-Size Scaling and Universality of the Thermal Resistivity of Liquid ^{4}He near T_λ

Daniel Murphy,[1] Edgar Genio,[1] Guenter Ahlers,[1] Fengchuan Liu,[2] and Yuanming Liu[2]
[1]*Department of Physics and iQUEST, University of California, Santa Barbara, California 93106*
[2]*Jet Propulsion Laboratory, California Institute of Technology, Pasadena, California 91109*
(Received 29 August 2002; published 13 January 2003)

We present measurements of the thermal resistivity $\rho(t, P, L)$ near the superfluid transition of ^{4}He at saturated vapor pressure and confined in cylindrical geometries with radii $L = 0.5$ and 1.0 μm [$t \equiv T/T_\lambda(P) - 1$]. For $L = 1.0$ μm measurements at six pressures P are presented. At and above T_λ the data are consistent with a universal scaling function $F(X) = (L/\xi_0)^{x/\nu}(\rho/\rho_0)$, $X = (L/\xi_0)^{1/\nu}t$ valid for all P (ρ_0 and x are the pressure-dependent amplitude and effective exponent of the bulk resistivity ρ, and $\xi = \xi_0 t^{-\nu}$ is the correlation length). Indications of breakdown of scaling and universality are observed below T_λ.

DOI: 10.1103/PhysRevLett.90.025301 PACS numbers: 67.40.Pm

The modern theory of critical phenomena [1] predicts that continuous phase transitions belong to distinct universality classes which are determined by such general properties of the system as the number of degrees of freedom of the order parameter and the spatial dimensionality. Within a given class, exponents and amplitude ratios are identical (i.e., universal) for all members and independent of irrelevant variables. An example of an irrelevant variable is the pressure P of a liquid helium sample at which measurements near the superfluid transition temperature T_λ are made. Within a given universality class, the dependence of many properties upon certain parameters can be represented by scaling functions which are the same for all systems. The present Letter is an experimental study of the scaling function which describes the effect of confinement in a cylindrical geometry with radius L on a transport property near a critical point [2,3]. For static properties this finite-size scaling has been studied by a number of precise experiments. For example, the heat capacity near the superfluid transition of ^{4}He has been measured for confinement sizes which vary by a factor of over 1000, and the data to a large extent can be collapsed upon a unique function when properly reduced [4–7]. Even for static properties, however, measurements which test the universality of such a scaling function are quite limited [8,9]. For transport properties there are, to our knowledge, no prior experiments which test scaling and universality for finite-size effects. There has been only one experiment on the effects of confinement on a transport property [10,11], namely, the measurements of the thermal conductivity λ of helium near T_λ in cylindrical tubes. These measurements can be used to derive a scaling function which would be expected to be universal, but since they were performed only for the one value $L = 1$ μm and only at saturated vapor pressure (SVP), they provided a test of neither finite-size scaling nor of the universality of the derived function.

We present experimental results for the thermal resistivity $\rho(t, P, L) \equiv 1/\lambda(t, P, L)$ near $T_\lambda(P)$ of liquid ^{4}He confined in cylinders of two different radii and at various pressures as a function of the reduced temperature $t \equiv T/T_\lambda - 1$. The use of two confinement sizes allows us to directly test finite-size scaling, while the use of different pressures for one size provides a test of universality. For bulk helium $\rho(t, P, \infty)$ depends strongly on pressure [12], so that a comparison of an appropriate scaling function for $\rho(t, P, L)$ at different pressures provides a sensitive test of universality. These two aspects were tested in separate experiments: measurements as a function of L were taken at SVP, and measurements as a function of P were taken at a single confinement size $L = 1.0$ μm.

Theoretical predictions for λ are still quite limited. Monte Carlo calculations give the shape of a scaling function, but only to within a multiplicative factor [13]. Within its precision this shape agrees well with the measurements of Ref. [10]. Very recently, a one-loop renormalization group (RG) calculation of $\lambda(t, P, L)$ for $t \geq 0$ and at SVP was carried out by Töpler and Dohm [14], but at present there are no such calculations for $t < 0$ and for higher pressures. Thus, in order to provide a broader framework for the analysis of our data, we use a phenomenological approach. We assume that the temperature and size dependence of ρ are separable and that the size dependence is a function only of L/ξ where $\xi = \xi_0 t^{-\nu}$ is the correlation length: $\rho(t, P, L) = \rho(t, P, \infty)\tilde{F}(L/\xi)$. Since $\rho(t, P, \infty)$ goes to zero as t does while $\rho(t, P, L)$ remains finite, $\tilde{F}$ diverges at $t = 0$. To avoid this difficulty, we redefine the scaling function as $F(X) = (L/\xi)^{x/\nu}\tilde{F}$, which avoids the divergence at $t = 0$. Consistent with experiment [12], we have written ρ for bulk helium as a power law $\rho(t, P, \infty) = \rho_0 t^x$ with effective exponents $x(P)$ and amplitudes $\rho_0(P)$. We now have

$$F(X) = \left[\frac{L}{\xi_0(P)}\right]^{x/\nu}[\rho(t, P, L)/\rho_0(P)], \tag{1}$$

with

$$X = \left(\frac{L}{\xi_0}\right)^{1/\nu} t. \tag{2}$$

The correlation length has a pressure-dependent amplitude $\xi_0(P)$ and a universal exponent ν. The values of ξ_0, ρ_0, and x are known from bulk measurements [12] and are summarized in Table I.

We used two different thermal conductivity cell types. Type I was described in detail elsewhere [10]. It was used for measurements of the resistivity as a function of P at $L = 1.0$ μm. It consisted of two cylindrical metal end plates made of oxygen-free high-conductivity copper separated by a stainless steel sidewall. A glass microchannel plate (MCP) was epoxied to the inside of the sidewall, so that when assembled the liquid helium between the plates would be confined to the channels with little extraneous liquid between the end plates and the glass. A small bulk thermal conductivity cell, called a "lambda device," was attached to the bottom (hot) copper plate for the determination of T_λ in bulk helium. The bottom of the lambda device was 1.25 cm below that of the confinement cell, and corrections for the hydrostatic pressure difference between the bottom of the lambda device and the middle of the MCP were made [15,16]. The cell was filled through an overflow volume located on the top (cold) copper plate.

Cell type II, used for measurements of the resistivity as a function of L at SVP, was designed for use with microchannel plates which were surrounded by a solid glass ring. Whereas the MCP in cell I was epoxied into a stainless steel sidewall which in turn was sealed to the copper end plates with indium gaskets, the glass ring in the second type was directly sealed to the copper end plates using indium. The cryogenic apparatus used with this cell design accommodated three thermal conductivity cells, all of which were suspended from a common temperature-regulated platform. One of these cells was a bulk conductivity cell constructed with a glass ring without microchannels in the central section. It served to locate T_λ of the bulk fluid. The conductivities of the three cells could be measured simultaneously. The fill lines entered the bottom of the cells, and the portion of the fill line located in the bottom end plate was packed with 0.05 μm alumina powder to suppress the superfluid transition. Thus the liquid helium contained in the bottom end plate was always normal. The fill line was connected to an overflow volume on the shield stage, which was maintained a few mK above T_λ.

Saturated vapor pressure was maintained in both sets of experiments by partially filling the overflow volumes. Pressures other than SVP were reached in cell type I using a "hot volume" [17], i.e., a separate thermal stage filled with fluid whose temperature was controlled so as to regulate the pressure in the thermal conductivity cell. The pressure was measured using a capacitative strain gauge [18] mounted on the top of the cell. The fluid in the cell and the hot volume was isolated from the rest of the cryostat by a normally closed low-temperature valve.

For cell I, the pressures at which measurements were made were chosen to match those for which prior measurements for bulk helium were available [12]. For all cells the resistivity ρ was computed from the temperature difference ΔT which was measured across the fluid layer when a power Q was applied to the bottom plate of a cell: $\rho = (A/d)[(Q/\Delta T - C_W)^{-1} - R_b]$, where A is the cross-sectional area of the fluid, d is the spacing between the plates, C_W is the parallel conductance of the stainless steel sidewall and the glass of the MCP, and R_b is the boundary resistance between the copper end plates and the fluid. The boundary resistance R_b was measured far below T_λ, where the resistance of the fluid layer can be neglected. The size of the correction is relatively small, and its temperature dependence near T_λ [19] was neglected. The parameters A/d and C_W were obtained by fitting the measured $\lambda(t, P, L)$ to the known $\lambda(t, P, \infty)$ several mK above T_λ where the effects of confinement are negligible. The value $d/\mathrm{A} = 0.386\ \mathrm{cm}^{-1}$ so obtained was found to be independent of pressure and agreed with the value $0.39\ \mathrm{cm}^{-1}$ previously determined for this cell [10]. The 0.5 and 1 μm data, taken with cell II, yielded $d/A = 0.0781$ and $0.0605\ \mathrm{cm}^{-1}$, respectively. All values for d/A are in good agreement with values from gas flow impedance measurements on and electron micrographs of

TABLE I. Values of the parallel conductance C_W and scaling function F at $X = 0$ versus pressure.

Cell	L (μm)	P (bars)	ξ_0 (nm)	$10^{-4}\rho_0$ (cm K/W)	x	$10^4 C_W$ (W/K)	$F(0)$
II	0.5	SVP	0.1432	8.312	0.4397	13.3	1.35
II	1	SVP	0.1432	8.312	0.4397	10.5	1.35
I	1	SVP	0.1432	8.312	0.4397	9.35	1.40
I	1	6.95	0.1425	9.073	0.4251	8.81	1.30
I	1	11.25	0.1410	10.19	0.4250	8.41	1.30
I	1	14.73	0.1399	11.10	0.4250	8.07	1.32
I	1	22.31	0.1382	12.79	0.4159	7.44	1.31
I	1	28.00	0.1314	15.07	0.4127	6.80	1.24

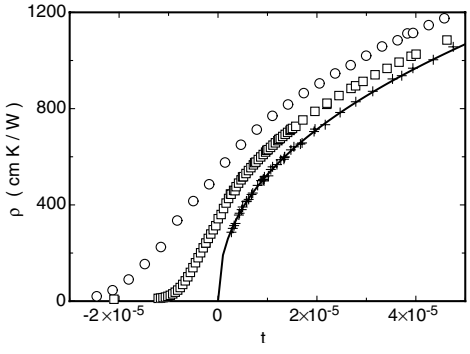

FIG. 1. Thermal resistivity versus reduced temperature at SVP for $L = 0.5$ μm (open circles) and 1.0 μm (open squares). The plusses are bulk measurements (Ref. [12]) and the solid line is a power-law fit to the bulk data.

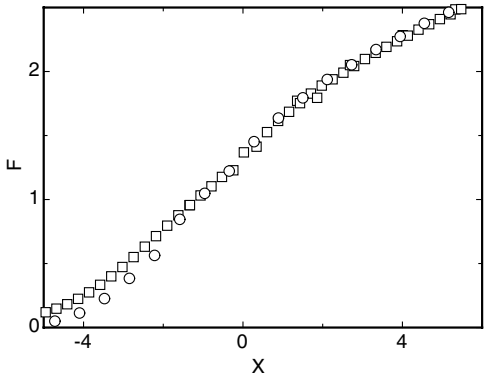

FIG. 2. Scaling function F versus scaling variable X at SVP for $L = 0.5$ μm (open circles) and 1.0 μm (open squares).

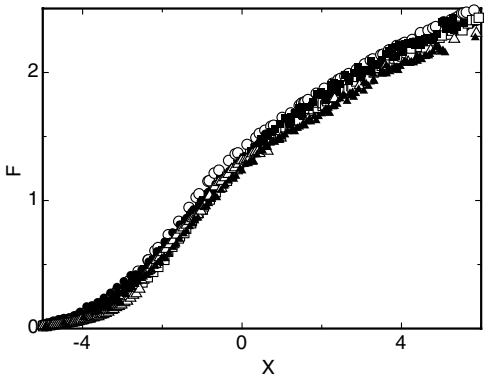

FIG. 4. Scaling function F versus scaling variable X for $L = 1.0$ μm. Pressures and symbols are as in Fig. 3.

the microchannel plates. The values for C_W for each size and pressure are shown in Table I (for $P = 11.25$ bars, there were no bulk conductivity data, and C_W was obtained by interpolation between other pressures). Each conductivity data point was assigned to the mean temperature $\bar{T} = T_{\text{top}} + \Delta T/2$, and a corresponding curvature correction [12] was applied to correct for the use of a finite Q and ΔT.

The resistivity at SVP is plotted versus t in Fig. 1 for two different values of L. The data show the effect of confinement, with the smallest size showing the greatest rounding of the transition and the greatest increase of $\rho(t = 0)$. The scaling variable $F(X)$ [Eq. (1)] is plotted versus X [Eq. (2)] for the two sizes in Fig. 2. Except for $X \lesssim -2$, the data collapse onto a single curve, thus supporting the concept of finite-size scaling. The small difference in F between the two data sets below $X \simeq -2$ suggests a breakdown of finite-size scaling in the superfluid phase.

Figure 3 shows $\rho(t, P, L)$ as a function of t for six different values of P and $L = 1.0$ μm. Whereas the resistivity of the bulk fluid drops to zero at $t = 0$ [12], that of the finite system remains finite at $t = 0$ and decreases smoothly to very small values as t becomes more negative. The value of $\rho(t = 0, P, L)$ varies by nearly a factor of 3 for the pressures used.

In Fig. 4 $F(X)$ is plotted versus X for six different pressures. Within the resolution of that figure and the experimental scatter, the data collapse onto the same curve, suggesting that a single scaling function describes all six pressures. The collapse occurs despite the large variation of ρ at constant t. The values of $F(X)$ at $X = 0$ are given in Table I.

The thermal conductivity λ is plotted on a logarithmic scale versus t on a linear scale in Fig. 5 for temperatures below $T_\lambda(P)$. It is consistent with an exponential growth below $T_\lambda(P)$ as noted previously [10]. The amplitudes and arguments of the exponential are approximately the same for all pressures. These results suggest that λ, rather than the scaling function F, becomes independent of pressure at low temperatures, and that universality breaks down below $T_\lambda(P)$. To explore this further, we show in Fig. 6 the scaling function $F(X)$ on a logarithmic scale as a function

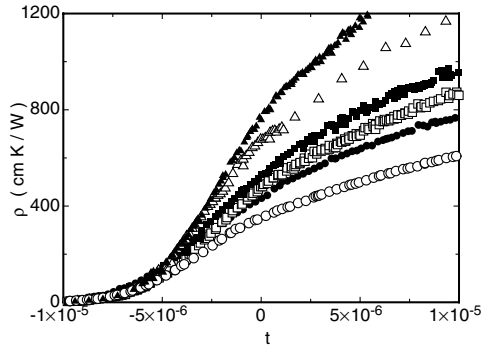

FIG. 3. Thermal resistivity versus reduced temperature for $L = 1.0$ μm at SVP (open circles); 6.95 bars (solid circles); 11.25 bars (open squares); 14.73 bars (solid squares); 22.31 bars (open triangles); 28.00 bars (solid triangles). The reduced temperature for each pressure is defined relative to $T_\lambda(P)$.

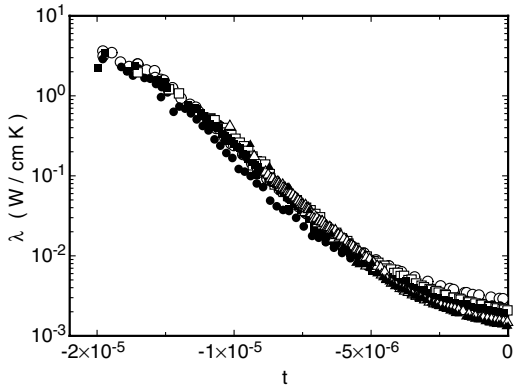

FIG. 5. The thermal conductivity below T_λ on a logarithmic scale versus reduced temperature on a linear scale for $L = 1.0$ μm. Pressures and symbols are as in Fig. 3.

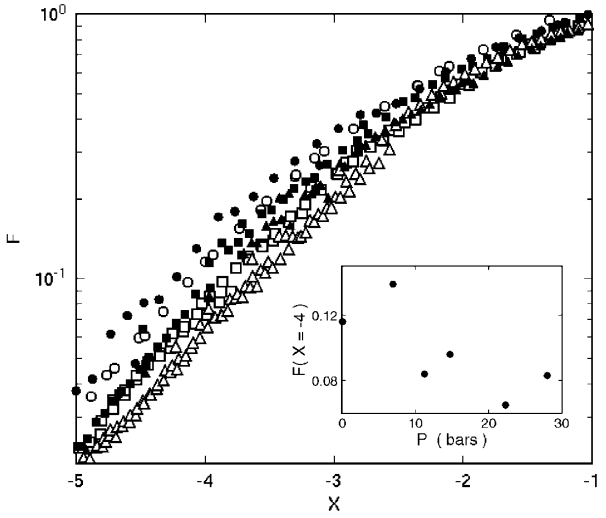

FIG. 6. The scaling function F below T_λ on a logarithmic scale versus X on a linear scale for $L = 1.0$ μm. Pressures and symbols are as in Fig. 3. The inset shows $F(X = -4)$ as a function of the pressure.

of X on a linear scale in the range below T_λ. For $X \gtrsim -2$ one sees that the data collapse within their resolution. However, at more negative X there is a systematic trend of $F(X)$ with P which exceeds the scatter of the data. This is seen from the inset in the figure, which gives F at $X = -4$ as a function of pressure. At $X = -4$ the results for $F(X)$ vary from about 0.13 at small P to about 0.07 at high P.

Aside from testing scaling and universality, an important issue is to what extent detailed theoretical calculations can reproduce the conductivity. As discussed above, the theoretical information is limited. Monte Carlo calculations, which give the shape of the scaling function quite well, involve as yet undetermined parameters [13]. However, the recent renormalization group calculations have yielded results for λ at SVP [14]. In Fig. 7 we show data for $\lambda(t = 0)$ as a function of L^{-1} on logarithmic scales. The phenomenological scaling function Eq. (1) predicts $\lambda(t = 0) \propto L^{-x/\nu}$ which, for $x/\nu = 0.656$, is shown by the solid straight line (the amplitude was adjusted to fit the data). The RG prediction is given by the dashed curve. It falls only about 15% below the data, and in the experimental range of L it has the same effective exponent (the slope of the curve) as the data and the scaling prediction. The excellent agreement with the RG calculation is particularly gratifying since all adjustable parameters in the theory are taken from properties of the bulk system and from static finite size properties [14].

Future plans call for the measurement of the resistivity at larger L, with the largest (50 μm) to be flown on the International Space Station. Those experiments will extend the range covered to two decades in L and will provide a much more severe test of the predictions.

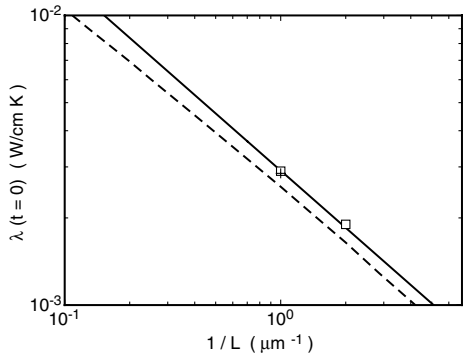

FIG. 7. Thermal conductivity $\lambda(t = 0)$ vs L^{-1} on logarithmic scales. The plus is the SVP measurement from cell I. Open squares are from cell II. The solid straight line is the prediction based on Eq. (1). The dashed curve is the prediction by Töpler and Dohm [14].

We thank Michael Töpler and Volker Dohm for sending us their results prior to publication. This work was supported by NASA Grant No. NAG8-1429.

[1] M. E. Fisher, Rev. Mod. Phys. **70**, 653 (1998).
[2] M. E. Fisher, in *Proceedings of the International School of Physics "Enrico Fermi,"* Course 51, edited by M. S. Green (Academic, New York, 1971).
[3] V. Privman, in *Finite Size Scaling and Numerical Simulations of Statistical Systems*, edited by V. Privman (World Scientific, Singapore, 1990).
[4] S. Mehta and F. M. Gasparini, Phys. Rev. Lett. **78**, 2596 (1997).
[5] S. Mehta, M. O. Kimball, and F. M. Gasparini, J. Low Temp. Phys. **114**, 467 (1999).
[6] M. O. Kimball, S. Mehta, and F. M. Gasparini, J. Low Temp. Phys. **121**, 29 (2000).
[7] J. A. Lipa, D. R. Swanson, J. A. Nissen, P. R. W. Z. K. Geng, D. A. Stricker, T. C. P. Chui, U. E. Israelsson, and M. Larson, Phys. Rev. Lett. **84**, 4894 (2000).
[8] M. O. Kimball and F. M. Gasparini, Phys. Rev. Lett. **86**, 1558 (2001).
[9] M. O. Kimball and F. M. Gasparini, J. Low Temp. Phys. **126**, 103 (2002).
[10] A. Kahn and G. Ahlers, Phys. Rev. Lett. **74**, 944 (1995).
[11] G. Ahlers, J. Low Temp. Phys. **115**, 143 (1999).
[12] W. Tam and G. Ahlers, Phys. Rev. B **32**, 5932 (1985).
[13] K. Nho and E. Manousakis, Phys. Rev. B **64**, 144513 (2001).
[14] M. Töpler and V. Dohm (to be published).
[15] G. Ahlers, Phys. Rev. **171**, 275 (1968).
[16] G. Ahlers, J. Low Temp. Phys. **84**, 173 (1991).
[17] K. Mueller, G. Ahlers, and F. Pobell, Phys. Rev. B **14**, 2096 (1976).
[18] G. Straty and E. Adams, Rev. Sci. Instrum. **40**, 1393 (1969).
[19] K. Kuehn, S. Mehta, H. Fu, E. Genio, D. Murphy, F. Liu, Y. Liu, and G. Ahlers, Phys. Rev. Lett. **88**, 095702 (2002).